THE JOURNAL OF BIOLOGICAL CHEMISTRY
Vol. 277, No. 18, Issue of May 3, pp. 15828–15833, 2002
Printed in U.S.A.

A Cross-linked Profilin-Actin Heterodimer Interferes with Elongation at the Fast-growing End of F-actin*

Received for publication, December 20, 2001, and in revised form, February 7, 2002
Published, JBC Papers in Press, February 13, 2002, DOI 10.1074/jbc.M112195200

Tomas Nyman‡, Rebecca Page§¶, Clarence E. Schutt§, Roger Karlsson‡, and Uno Lindberg‡‖

From the ‡Department of Cell Biology, the Wenner-Gren Institute, Stockholm University, S-106 91 Stockholm, Sweden and the §Department of Chemistry, Henry H. Hoyt Laboratory, Princeton University, Princeton, New Jersey 08544

Profilin and β/γ-actin from calf thymus were covalently linked using the zero-length cross-linker 1-ethyl-3-(3-dimethylaminopropyl)-carbodiimide in combination with *N*-hydroxysuccinimide, yielding a single product with an apparent molecular mass of 60 kDa. Sequence analysis and x-ray crystallographic investigations showed that the cross-linked residues were glutamic acid 82 of profilin and lysine 113 of actin. The cross-linked complex was shown to bind with high affinity to deoxyribonuclease I and poly(L-proline). It also bound and exchanged ATP with kinetics close to that of unmodified profilin-actin and inhibited the intrinsic ATPase activity of actin. This inhibition occurred even in conditions where actin normally forms filaments. By these criteria the cross-linked profilin-actin complex retains the characteristics of unmodified profilin-actin. However, the cross-linked complex did not form filaments nor copolymerized with unmodified actin, but did interfere with elongation of actin filaments in a concentration-dependent manner. These results support a polymerization mechanism where the profilin-actin heterodimer binds to the (+)-end of actin filaments, followed by dissociation of profilin, and ATP hydrolysis and P_i release from the actin subunit as it assumes its stable conformation in the helical filament.

Profilin, originally isolated as a 1:1 complex with β-actin (1, 2), is an essential actin-binding protein involved in the control of actin filament formation *in vivo* (see Refs. 3 and 4, and references therein). The profilin-actin complex is unable to nucleate filament formation *in vitro*, but is suggested to interact with the (+)-end (barbed end) of preexisting filaments (5–10), resulting in the dissociation of the profilin-actin complex and incorporation of actin monomers into filaments. The (−)-end (pointed end) of actin filaments, does not bind profilin-actin (5, 6, 11). This behavior of the complex is explained by the orientation of the actin protomers in the actin filament giving it polarity (12), by the location of the profilin binding site on actin (13), and the strength of the profilin-actin interaction (6, 9). Profilin binds to the (+)-end of the actin monomer leaving the (−)-end free to interact with the (+)-end of actin nuclei or filaments. Consequently, in the presence of (+)-end capping agents like members of the gelsolin family, profilin efficiently sequesters actin monomers and causes depolymerization of actin filaments.

Profilin greatly lowers the affinity for both ATP and divalent cation on actin, thereby increasing their exchange rates (14–16). It has been suggested that this effect of profilin on actin might be important *in vivo* during conditions of rapid filament turnover, when the exchange of ADP for ATP otherwise might be rate-limiting (16).

To learn more about the nature of the profilin-actin complex and its significance in the actin polymerization process, a covalently cross-linked profilin-β/γ-actin complex (PxA)[1] was produced. The value of PxA as a tool for *in vivo* studies of the profilin-actin complex was illustrated in a recent report describing the effects on the organization of the microfilament system of cultured cells by microinjected PxA (17).

The present study describes the preparation of PxA, the evaluation of its structural characteristics, and its use in studies of actin filament formation from profilin-actin *in vitro*. The PxA complex retained the capacities of wild type profilin-actin (PA) to bind DNase I and poly(L-proline) (PLP), and to bind and exchange nucleotide with kinetics close to that of PA. This indicates that the surface structure of PA was conserved all through the cross-linking reaction. The PxA complex did not hydrolyze ATP even under actin-polymerizing conditions (1 mM $MgCl_2$, 100 mM KCl), and it could neither polymerize nor participate in filament formation from unmodified actin. It did, however, interfere with the formation of actin filaments, indicating that it retained the capacity to interact with the (+)-end of growing filaments. These results are discussed in comparison with a differently cross-linked profilin-actin complex (18). Crystallographic analysis showed PxA to be closely similar to unmodified profilin-actin.

MATERIALS AND METHODS

Preparation of Profilin and Actin—Profilin I and β/γ-actin were isolated as a complex from calf thymus using poly(L-proline)-affinity and hydroxyapatite chromatography (Hypatite C, even lot number, Clarkson Chromatography Products, South Williamsport, PA). Actin was subsequently separated from profilin by polymerization and sedimentation of the filaments. Filamentous actin was depolymerized by extensive dialysis and finally gel-filtered using Sephacryl S-300 (Amersham Biosciences AB, Uppsala, Sweden) equilibrated with buffer G (0.5 mM Tris, 0.5 mM ATP, 0.1 mM $CaCl_2$, 0.5 mM DTT, pH 7.6 at room temperature). Profilin was further purified by DEAE ion-exchange chromatography (19, 20).

* This work was supported by the Swedish Natural Science Research Council (to U. L. and R. K.), the Swedish Foundation for International Cooperation in Research and Higher Education (to U. L.), and Grant GM44038 from the National Institutes of Health (to C. E. S.). The costs of publication of this article were defrayed in part by the payment of page charges. This article must therefore be hereby marked "*advertisement*" in accordance with 18 U.S.C. Section 1734 solely to indicate this fact.

¶ Present address: Scripps Research Inst., La Jolla, CA 92037.
‖ To whom correspondence should be addressed. E-mail: uno@cellbio.su.se.

[1] The abbreviations used are: PxA, covalently cross-linked profilin-β/γ-actin complex; εATP, 1,N^6-ethenoadenosine 5′-triphosphate; EDC, 1-ethyl-3-(3-dimethylaminopropyl)-carbodiimide; NHS, *N*-hydroxysuccinimide; CNS, crystallography NMR software; PA, profilin-actin; DTT, dithiothreitol; HPLC, high performance liquid chromatography; PLP, poly(L-proline).

Cross-linking Reaction—The cross-linking procedure was developed from Ref. 21. Profilin was transferred to buffer A (0.1 mM $CaCl_2$, 10 mM HEPES, pH 7.5) by Sephadex G-25 chromatography and diluted to 2 mg/ml. To form reactive esters on profilin, EDC and sulfo-NHS (Pierce) were added to 6 and 15 mM, respectively, and the mixture was left for 20 min in room temperature. Meanwhile, actin was transferred to buffer X (0.1 mM ATP, 0.1 mM $CaCl_2$, 0.5 mM DTT, 10 mM HEPES, pH 7.5) and diluted to 1 mg/ml. The activation of profilin was interrupted and any unreacted EDC destroyed by the addition of DTT to 20 mM (22). The activated profilin was mixed with an equal volume of ice-cold actin and the mixture was immediately filtered through Sephadex G-25 equilibrated with buffer X. This step removed excess NHS and the urea derivative resulting from hydrolysis of EDC. The mixture was left on ice overnight. Profilin-actin was isolated from excess profilin by gel filtration on a Sephacryl-300 (Amersham Biosciences AB) column equilibrated with buffer G.

Determining the Site of Cross-linking—PxA and PA were digested with 4 μg/ml endoproteinase Glu-C (V8 protease, EC 3.4.21.19; Sigma) in the presence of 4 M urea, at 0 °C for 72 h. Subsequent SDS-PAGE analysis resulted in the isolation of two PxA-specific fragments. After electrotransfer to nitrocellulose, the heavier fragment was excised and submitted to microsequencing (Applied Biosystems Inc. model 476A). This led to the determination of the cross-linked residue in the actin sequence (see "Results"). The naturally acetylated N terminus of the profilin-derived part of the PxA-specific fragments was assumed to be intact and hence blocked for Edman degradation. Therefore, the excised nitrocellulose piece was further treated with proteinase Asp-N (Roche Molecular Biochemicals, sequencing grade 1054589) in the presence of 1 M guanidinium HCl. The resulting peptides were separated on HPLC (Amersham Biosciences Smart equipped with a Vydac C18 1 × 250-mm column), and microsequenced as above.

DNase I Binding—The dissociation constant of the actin-DNase I interaction was determined from double-reciprocal plots of the dependence of DNase I inhibition on actin concentration, measured at 25 °C using the DNase I inhibition assay (23, 24).

Binding to Poly(L-proline)—From a poly(L-proline)-Sepharose suspension, prepared as in Ref. 19, 100 μl were transferred to two 1.5-ml Eppendorf tubes. The Sepharose was pelleted by a brief centrifugation, washed with 500 μl of buffer G, and re-pelleted. The supernatant was discarded, leaving a Sepharose pellet of 50 μl. To each pellet was added 18 nmol of either PxA or PA in a total volume of 100 μl (buffer G). After mixing and incubation at room temperature for 10 min, the poly(L-proline)-Sepharose was again pelleted and the amount of unbound protein in the resulting supernatant was determined using the Bradford protein determination assay.

ATP Exchange—PxA and PA were freed from excess nucleotide by gel filtration over a small Sephadex G-25 column (PD10, Amersham Biosciences AB) equilibrated with ATP-free buffer G. The protein concentration was adjusted to 6.5 μM, and after addition of 300 μM ϵATP (Molecular Probes, Eugene, OR), the fluorescence increase at >408 nm (excitation at 360 nm) was monitored using a Sigma ZWS II spectrofluorometer (Biochem Wissenschaftliche Geräte GmbH, Puchheim, Germany). Under these conditions, re-binding of ATP is negligible, and the rate of incorporation of ϵATP represents k_{-ATP}, the off-rate for ATP (*e.g.* Ref. 25). Off-rates for ATP were estimated by first-order curve fitting of the experimental data using Origin (Microcal Software Inc., Northampton, MA).

Polymerization Experiments—Sedimentation and SDS-PAGE analysis of the polymerizability of PxA was performed as follows. Solutions of 0.5 mg/ml PxA with, or without, 0.5 mg/ml β/γ-actin was prepared. The high affinity bound Ca^{2+} was replaced with Mg^{2+} by incubation in 0.2 mM EGTA and 50 μM $MgCl_2$ for 10 min. Filament formation was induced by the addition of $MgCl_2$ and KCl to final concentrations of 1 and 100 mM, respectively. Following incubation for 1 h at room temperature and centrifugation at 100,000 × *g* for 20 min, the original mixtures, the supernatants, and the pellets were analyzed by gel electrophoresis.

Viscometry was performed using a Cannon-Manning viscometer with a buffer flow time of 56 s at 25 °C, and with a sample volume of 0.7 ml. PxA and PA were mixed to increasing ratios, keeping the concentration of unmodified profilin-actin constant at 9 μM. After replacing the high affinity bound Ca^{2+} with Mg^{2+} as above, the reaction mixture was supplemented with 1 mM $MgCl_2$ and 100 mM KCl. The viscosity of the sample was then measured every 2 min.

ATP Hydrolysis—Measurements of the ATPase activity was performed at 25 °C and in the presence of 1 mM $MgCl_2$ and 100 mM KCl. At concentrations of 9 μM, cross-linked and unmodified profilin-actin was incubated with [γ-^{32}P]ATP (0.1 mCi/ml), 0.2 mM EGTA, and 50 μM $MgCl_2$ for 10 min at room temperature. This allowed replacement of CaATP by MgATP. After addition of 1 mM $MgCl_2$ and 100 mM KCl, the increase in concentration of inorganic phosphate (P_i) was followed by the phospho-molybdate precipitation assay (26, 27).

Crystallization—The PxA complex was crystallized in complex with either CaATP or MgATP, largely adopting the procedure previously used for profilin-β-actin (19, 28). For CaATP-PxA, 5–8 mg/ml purified PxA was supplemented with 0.5 mM $CaCl_2$ and 0.1 mM EDTA and dialyzed against buffer C_{Ca} (1.3 M KPO_4, pH 7.3, 0.5 mM ATP, 0.5 mM $CaCl_2$, 0.1 mM EDTA, 2.0 mM DTT) for a minimum of 8 h in 4 °C. For MgATP-PxA, CaATP-PxA from the same batch was supplemented with 0.5 mM $MgCl_2$ and 0.5 mM EGTA and dialyzed against buffer C_{Mg} (1.3 M KPO_4, pH 7.3, 0.5 mM ATP, 0.5 mM $MgCl_2$, 0.5 mM EGTA, 2.0 mM DTT). A small amount of precipitate formed during dialysis was pelleted by centrifugation for 10 min at 100,000 × *g*, 4 °C. The clarified solution was filtered through a 0.2-μm filter (DynaGard, Microgon Inc., Laguna Hills, CA). Crystallization was done using the hanging drop technique. Drops of 10 μl were set up with the corresponding buffer C in the well. From drops of unfiltered protein solution, microcrystals rapidly formed. These were collected, crushed, and sonicated in the respective buffer C. The resulting solution was briefly centrifuged, and the top part was used to microseed hanging drops of the filtered PxA solutions. Crystals of both magnesium- and calcium-complexed PxA typically grew to their full size within 36 h. Crystals were harvested and transferred to buffer C (magnesium or calcium) containing 1.8 M K-PO_4, pH 7.3.

Synchrotron x-ray data were collected at beamline x12c at the National Synchrotron Light Source (NSLS) facility in Brookhaven, NY. The Mg-PxA crystals were cooled in liquid nitrogen after soaking (5–10 s) in buffer C containing 25% glycerol as cryoprotectant. Data collection was done at 100 K. Data were reduced and scaled using Denzo and Scalepack (29). Initial rigid body refinement was done using CNS with the open-state profilin-β-actin structure (Protein Data Bank access code 1HLU) as a search model.

RESULTS

Production of Cross-linked Profilin-β/γ-Actin—To cross-link profilin and actin, the procedures where the cross-linking reagents were mixed either with profilin-actin or with actin prior to the addition of profilin were first applied (18, 30). These approaches resulted in the formation of actin oligomers (dimers, trimers, etc.), and 5–20% of the starting amount of actin appeared as cross-linked profilin-actin heterodimer (data not shown). However, when profilin was activated with the reagent prior to addition of actin, as described under "Materials and Methods," typically more than 90% of the actin in the reaction mixture was cross-linked to profilin and only trace amounts of oligomers formed, as judged by SDS-PAGE (Fig. 1). The cross-linked product, PxA, eluted as a single peak from an S-300 gel filtration column together with unreacted profilin-actin, well separated from excess profilin (Fig. 1).

Identification of Cross-linked Residues—The cross-linking reagents used, EDC and NHS, react predominantly with solvent-exposed carboxyl groups, *i.e.* Asp and Glu residues, and C termini of proteins, yielding reactive succinimidyl esters. In the cross-linking reaction, these activated carboxyl groups react with primary amino groups, most often the ϵNH_2 of lysins (21). In the reaction, the NHS is reformed and the final product is an amide bond linking the two side-chains. Because of the polarity of the reaction, different protocols can generate different cross-links between the reacting proteins. Because the procedure used here differs from those described earlier (18, 30), it was unlikely to result in the same cross-linked residues.

To determine the site of cross-linking, PxA and PA were proteolytically digested with endoproteinase Glu-C, and analyzed by SDS-PAGE. Two PxA-specific proteolytic fragments with apparent molecular masses of 17–18 kDa and clearly larger than profilin were observed (Fig. 2). The peptides were electroblotted, and the two fragments were excised and subjected to sequence analysis. The results showed that both fragments had only one detectable sequence starting with the same N terminus. Sequence analysis of the upper fragment revealed

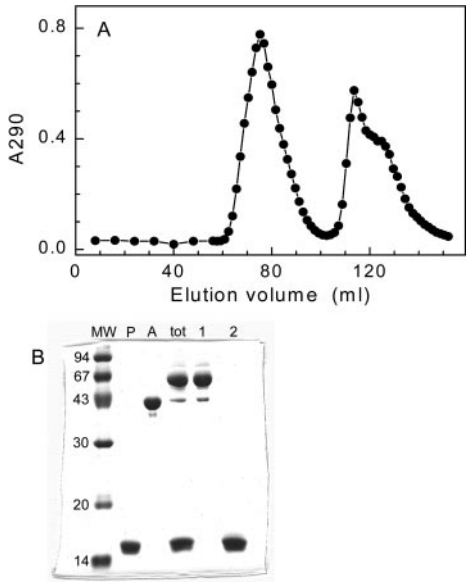

FIG. 1. **Isolation of covalently cross-linked PxA.** *A*, the reaction mixture was submitted to chromatography on a Sephacryl S-300 column. *B*, SDS-PAGE analysis of the isolated material. Samples from *left* to *right*: molecular weight marker (*MW*), profilin (*P*), actin (*A*), the reaction mixture prior to chromatography (*tot*), and samples from the first (*1*) and second (*2*) peak. The material in the first peak, containing PxA and trace amount of PA, was concentrated and kept on ice.

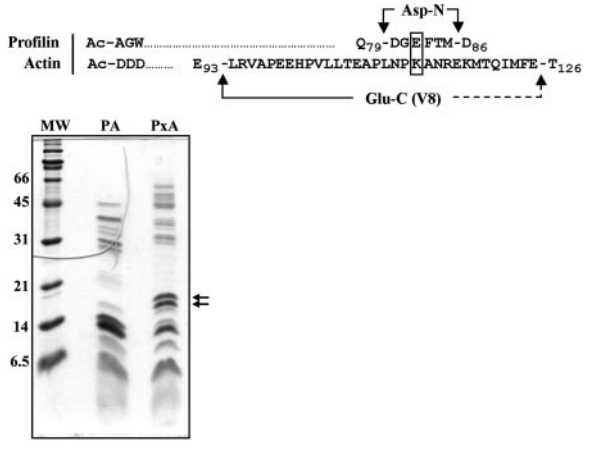

FIG. 2. **Proteolysis and sequence analysis.** The SDS-PAGE gel displays the proteolytic fragments resulting from treatment of PA and PxA with Glu-C (V8 protease). Two PxA-specific bands appeared (*arrows*). The upper band was submitted to further proteolysis and sequence analysis. The *scheme* shows the discussed proteolytic cleavage sites within the profilin and actin sequence. The *dashed arrow* (*right*) points at a putative cleavage site not confirmed by sequence analysis. The cross-linked residues Glu-82 and Lys-113 are *boxed*. Note that bovine profilin and actin are N-terminally acetylated.

the sequence LRVAPEEHPVLLTEAPLNPKANREK . . . , corresponding to residues 94–118 in actin. The yield in the sequencing steps after Pro-112 decreased abruptly suggesting that Lys-113 (underlined) was involved in the cross-link. There was no detectable profilin sequence, suggesting that the profilin fragment of the sample contained the acetylated N terminus.

To determine the profilin residue involved in the cross-link, the upper band material generated by Glu C proteinase was further digested with endoproteinase Asp-N (Fig. 2). The resulting peptides were fractionated by HPLC, and subsequent microsequence analysis identified a peak that contained two N termini available for sequencing. Residues LRVAPEEHPVLL . . . were found and identified as residues 94–105 of

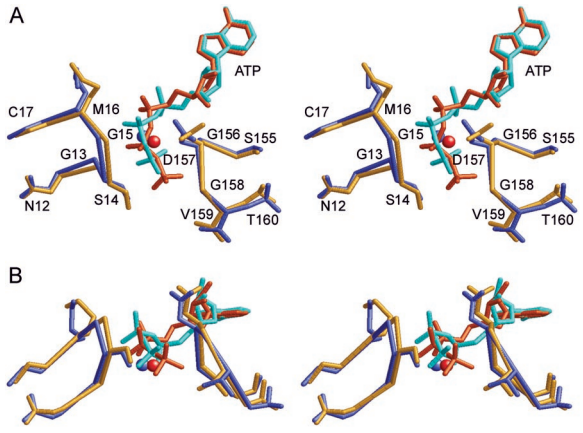

FIG. 3. **Comparison of the nucleotide binding sites of PxA and the profilin-actin open state.** The stereo images show the nucleotide and the phosphate-binding loops viewed down the interdomain cleft (*A*) and from the side (*B*). Profilin-actin is shown in *blue* and *cyan* (ATP), and PxA in *yellow* and *orange* (ATP). The image was generated using RasMol (52).

actin. A parallel sequence of residues, DGEFTM, was identified as profilin residues 80–85. The first two residues, Asp-80 and Gly-81, were obtained in good yields, whereas Glu-82 to Met-85 gave weak but identifiable signals, suggesting that Glu-82 was involved in the cross-link. This supported the prediction made from studies of the profilin-β-actin crystal structure that the two molecules should be coupled via Lys-113 of actin and Glu-82 of profilin, and this prediction was also strongly supported by x-ray crystallography (see below).

Crystallization of PxA—Incubation of unmodified profilin-actin at polymerizing KCl concentrations with Ca^{2+} as the high affinity bound divalent cation does not give rise to filaments (31). Exchanging Ca^{2+} for Mg^{2+}, however, results in filament formation. This is interesting because, under nonpolymerizing conditions, there appears to be little or no difference in the K_d of the profilin-actin interaction depending on the divalent cation (8–10), suggesting that Mg^{2+} in polymerizing concentrations of KCl introduces a structural change in the actin, facilitating nucleation and subsequent elongation of filaments. The fact that filaments form from PA in the presence of Mg^{2+} has precluded the crystallization of the complex under these conditions. The availability of the nonpolymerizing PxA provided the possibility to determine the structure of profilin-actin both in the calcium and magnesium form.

Complexes of PxA plus CaATP or PxA plus MgATP crystallized readily in buffer conditions previously used with profilin-β-actin and profilin-γ-actin (13, 19, 28). The crystals resembled the earlier described profilin-actin crystals, belonging to the space group $P2_12_12_1$, and having unit cell dimensions a = 37.6, b = 71.4, c = 182.7 Å. Depending on the buffer conditions, the c dimension of unmodified profilin-β-actin crystals varies between 172.7 and 185.7 Å, representing a closed and an open conformation of the nucleotide binding cleft (28). The crystallographic structures of profilin-actin and PxA are closely similar, as illustrated in the comparison of the nucleotide binding sites of the two structures (Fig. 3). Electron density maps of the MgATP-PxA complex clearly displayed the cross-link between Glu-82 and Lys-113 in a region of high order (Fig. 4), supporting the results from sequence analysis.

Biochemical Characteristics of PxA—Inhibition of the endonuclease activity of DNase I is a sensitive test of the three-dimensional structure of actin (32). DNase I binds to the (−)-end of actin, whereas profilin binds to the (+)-end, and the DNase I inhibiting activity of actin is not affected by the presence of profilin (32). Therefore, the DNase I inhibiting activity

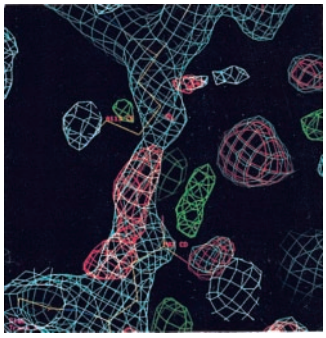

FIG. 4. **Electron density map showing the cross-linked residues Lys-113 of actin and Glu-82 of profilin.** Residue Lys-113 protrudes downward from the backbone density seen in the upper part of the image. Residue Glu-82 extends upward from the lower half. The structure was phased by molecular replacement using the open-state profilin-β-actin structure as a search model (Protein Data Bank code 1HLU). The simulated annealing omit map was calculated using CNS after a single round of rigid body refinement in which actin and profilin were allowed to refine independently. The image was made using the program O (51).

of PxA was investigated as a test of the intactness of the (−)-end of the actin in the cross-linked complex. The analysis showed that PxA bound DNase I almost as tightly as free actin, with a K_d of 2.3 nM, as compared with 1.0 nM for free actin.

Profilin and profilin-actin bind PLP with high affinity (19, 33). As reported previously, cross-linking profilin to actin as described here did not significantly alter the profilin-PLP interaction (17). Because the PLP binding site involves both the N- and the C-terminal helices of profilin (34, 35), the interaction of PA with PLP is strong evidence for the profilin being correctly folded.

Profilin reduces the affinity of actin for both the divalent cation and the nucleotide, resulting in a drastic increase in the rate of nucleotide exchange (14–16, 36). The CaATP dissociation characteristics of PxA were examined using the fluorescent ATP analogue ϵATP. The ATP dissociation rate constant (K_{-ATP}) determined for PxA was 0.075 ± 0.007 s^{-1} as compared with 0.069 ± 0.006 s^{-1} for the unmodified profilin-actin complex. These rate constants are in good agreement with previously reported dissociation rate constants for the interaction between ATP and bovine profilin-α-actin (16).

These observations show that the biochemical and structural characteristics of PA remained largely unaltered through the cross-linking reaction.

Polymerizability of PxA—Sedimentation and SDS-PAGE analysis indicated that PxA could not form filaments in the presence of $MgCl_2$ and KCl, not by itself nor together with actin (Fig. 5). Polymerization from PA as seen by viscometry showed that the rate of polymer formation was inhibited by PxA in a concentration-dependent manner (Fig. 6). At a 1:1 ratio of PxA to PA, the time to reach half-maximal viscosity was prolonged from 8 to 14 min and the maximal rate of change in viscosity was decreased by 41%. This indicated competition between PA and PxA for elongation at the filament (+)-ends. The final level of viscosity was not significantly affected by increasing concentrations of PxA, suggesting that PxA interacted transiently with filament (+)-ends.

ATPase—Profilin inhibits the intrinsic ATP hydrolyzing activity of G-actin (37). Because the PxA complex is unable to polymerize, it provided an opportunity to examine the intrinsic ATPase activity of profilin-bound actin at high (polymerizing) salt concentrations. It was found that, in 100 mM KCl and 1 mM $MgCl_2$, where PA normally contributes to polymer formation, PxA did not hydrolyze ATP (Fig. 7). This implies that, in addition to increasing the rate of nucleotide exchange on actin,

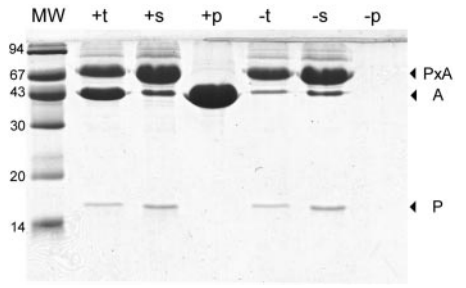

FIG. 5. **Sedimentation and SDS-PAGE analysis of the polymerizability of PxA.** PxA was incubated with 1 mM $MgCl_2$ and 0.1 M KCl, in the presence (+) or absence (−) of 0.5 mg/ml β/γ-actin. Following incubation and ultracentrifugation, the starting mixtures (*t*), the supernatants (*s*), and the pellets (*p*) were analyzed by gel electrophoresis.

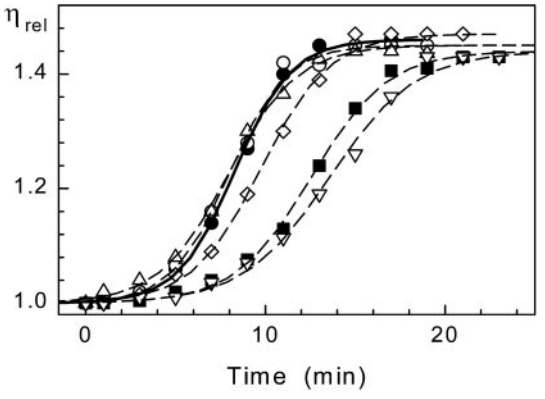

FIG. 6. **Viscometry analysis of the influence of PxA on actin polymerization.** Cross-linked profilin-actin was added in increasing amounts to samples containing 9 μM non cross-linked PA. The high affinity bound Ca^{2+} was replaced by Mg^{2+}, and polymerization was induced by the addition 0.1 M KCl and 1 mM $MgCl_2$. The *symbols* denote ratios of PA/PxA as follows: *filled circles* and *solid line*, 1/0; *open circles*, 1/0.2; *rightside-up triangles*, 1/0.4; *diamonds*, 1/0.6; *squares*, 1/0.8; *upside-down triangles*, 1/1.

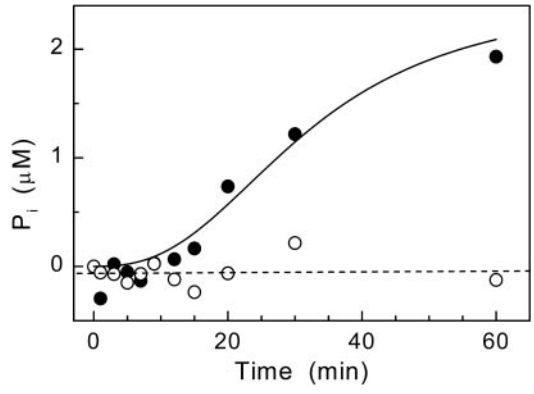

FIG. 7. **The ATPase activity of cross-linked and unmodified profilin-actin.** Cross-linked (*open circles*) and non-cross-linked (*closed circles*) profilin-actin was incubated with [γ-^{32}P]ATP (0.1 mCi/ml), 0.2 mM EGTA, and 50 μM $MgCl_2$ for 10 min at 25 °C. After addition of 1 mM $MgCl_2$ and 100 mM KCl, the formation of inorganic phosphate (P_i) was followed by the phospho-molybdate precipitation assay (26, 27).

the presence of profilin ensures that actin-bound ATP remains unhydrolyzed.

DISCUSSION

As shown here, the structure and biochemical characteristics of PxA are closely similar to those of unmodified PA with the exception that it does not polymerize.

Intrinsic ATPase Activity—Actin binds ATP tightly in complex with a divalent cation (38, 39). Under nonpolymerizing conditions, the ATP is slowly hydrolyzed, an activity that ap-

pears to be intrinsic to the actin monomer and not dependent on dimer formation (40, 41). Replacing Ca^{2+} by Mg^{2+} at the high affinity divalent cation binding site lowers the rate of nucleotide exchange and enhances the intrinsic ATPase activity (25, 42, 43). This may be related to the observation that Mg^{2+} induces a structural change, probably the closing of the interdomain cleft, that protects the region around Lys-68 in the interdomain cleft from proteolytic attack (44).

The binding of profilin to actin counteracts this Mg^{2+} effect in that it greatly lowers the affinity for the nucleotide on actin, increasing its rate of exchange (14–16). The explanation for this is found in the flexibility of actin in the interdomain region that allows opening and closing of the nucleotide-binding cleft (13, 28). Shear motions involving the interdomain Gln-137–Ser-145 helix connecting subdomains 1 and 3 bring about a 2.8° rotation of subdomain 1 that results in an outward shift of the Asn-12–Cys-17 loop, exposing the ATP phosphate tail to solution (28, 45). Importantly, the tight-to-open state transition disrupts divalent cation coordination with amino acid residues in the cleft: Asp-11 and Asp-154 in subdomains 1 and 3, respectively; and Gln-137 in the shearing helix. The profilin binding site on actin spans these subdomains on the (+)-end of the monomer, on the opposite side of the interdomain helix relative to the nucleotide binding cleft. This explains how the binding of ATP to actin depends on the divalent cation (25, 46), and how profilin might enhance nucleotide dissociation by disrupting cation coordination (42). The findings that profilin inhibits ATP hydrolysis on the actin monomer, under nonpolymerizing conditions (37) as well as under polymerizing conditions as shown here, supports the view that profilin-actin is in an open state conformation under physiological salt concentrations, even in the presence of Mg^{2+}.

Filament Formation from PA and the Structure of F-actin—Earlier studies suggested the possibility that PA might interact directly with the (+)-end during filament formation (5–8, 47). This view was supported by determination of free unpolymerized actin under steady state polymerizing conditions in the presence of mutant profilins with varying affinity for actin (9). The present investigation demonstrates that PxA interferes with both nucleation and elongation phases of the polymerization reaction of actin in the presence of non-cross-linked material. This indicates that the PA complex can bind to the (+)-end of actin nuclei and filaments, and, unless profilin dissociates so as to allow the final annealing of its ferried actin monomer, the incorporation is aborted and the complex dissociates from the growing filament.

Because profilin inhibits ATP hydrolysis on actin, profilin release during polymer formation from PA must occur prior to ATP hydrolysis. This implies that the initial binding of native PA to the (+)-end of actin filaments induces a conformational change in actin that promotes the dissociation of profilin. In this model, the ensuing ATP hydrolysis and P_i release are coupled to further structural changes during which the actin subunit adopts its final F-actin conformation.

Recently, a covalently cross-linked complex comprising profilin and rabbit α-actin, denoted PA_{cov}, was described (18). This complex was obtained by activating actin with the EDC/NHS reagent prior to the addition of profilin. Based on an earlier report on the covalent coupling of *Acanthamoeba* profilin and actin, shown to involve Lys-115 of profilin and Glu-364 of actin (30), the cross-link of PA_{cov} was assumed to engage Lys-125 of profilin (corresponding to K115 in the amoeba profilin) and Glu-364 of actin. The alternative protocol used here linked Glu-82 of profilin to Lys-113 of actin. The two complexes, PA_{cov} and PxA, behave differently in that PA_{cov} can form filaments by itself, or together with uncomplexed actin, whereas PxA cannot. It was argued (18) that the formation of helical filaments from PA_{cov} is not predicted by the Holmes/Lorenz F-actin model (48, 49) because PA_{cov} would not only interfere with the formation of the long-pitch helix, but should cap actin filaments at their (+)-end. Alternatively, if the actin ribbon structure found in the profilin-actin crystals is an assembly intermediate in the formation of F-actin (13), converting to an F-actin helix upon release of profilin (50), then PA_{cov} should form nonhelical profilin-actin ribbons, according to these authors (18). Instead, it was found that PA_{cov} formed filaments with the same helical periodicity as native F-actin.

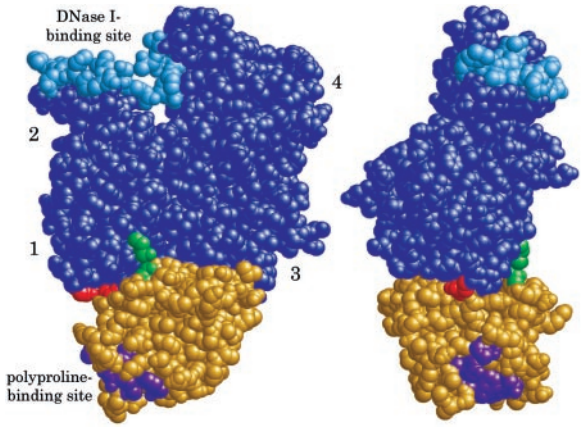

FIG. 8. **The different cross-links.** The cross-linked residues in PxA, Glu-82 of profilin and Lys-113 of actin, are shown in *green*, whereas the earlier reported cross-link involving Lys-125 of profilin (Lys-115 of *Acanthamoeba* profilin) and Glu-364 in actin (30), is shown in *red*. In the *left image*, actin is oriented with subdomain 1 to the *lower left*. The image was made using the program RasMol (52) and the profilin-β/γ-actin complex (Protein Data Bank access code 2BTF) (13).

However, it should be noted that actin amino acid residue, Glu-364, involved in the PA_{cov} cross-link is located in a turn near the actin C terminus at the outer "edge" of subdomain 1, in a region known to be flexible and particularly sensitive to polymerization conditions (Fig. 8). During incorporation of PA_{cov}, at the (+)-end of an actin filament, it is conceivable that the tethered profilin detaches from its interfacial contact with actin and swings out to the side of the filament. This movement exposes the (+)-end of the filament for interaction with an incoming PA_{cov} heterodimer. Thus, the Holmes/Lorenz model of F-actin and also profilin-actin ribbon-based models are compatible with the observation that PA_{cov} can form normally appearing F-actin filaments.

The difference between PA_{cov} and PxA in the ability to form filaments most likely arises from differences in the freedom of profilin to shift in position relative to actin during the interaction with actin nuclei or polymers. As discussed above, in the case of PA_{cov}, such shifts might enable normal polymerization reactions, involving the release of profilin from (+)-end assembly intermediates. In the case of PxA, the cross-linked residue, Lys-113, protrudes from the center of subdomain 1, a region not expected to be unusually flexible. Thus, for PxA, in contrast to PA_{cov}, the position of the cross-link apparently prevents the dislocation of profilin and subsequent incorporation of the actin subunit into the filament, aborting the assembly at the intermediate stage.

The observation that PA_{cov} forms helical filaments with the same periodicity as native F-actin is most interesting, because it would seem to provide an opportunity to determine the orientation of the actin monomer in F-actin. This is important, because the monomer orientation in the Holmes/Lorenz model of F-actin differs from that in the actin ribbon found in the profilin-actin crystals. Reconstructions of PA_{cov} filaments from

electron micrographs may reveal the location of Glu-364 of actin relative to the filament axis accurately enough to discriminate between the two cases.

Acknowledgment—We are grateful to Bob Sweet at NSLS for kindly providing beam time.

REFERENCES

1. Carlsson, L., Nyström, L. E., Lindberg, U., Kannan, K. K., Cid-Dresdner, H., and Lövgren, S. (1976) *J. Mol. Biol.* **105,** 353–366
2. Carlsson, L., Nyström, L. E., Sundkvist, I., Markey, F., and Lindberg, U. (1977) *J. Mol. Biol.* **115,** 465–483
3. Sohn, R. H., and Goldschmidt-Clermont, P. J. (1994) *Bioessays* **16,** 465–472
4. Schlüter, K., Jockusch, B. M., and Rothkegel, M. (1997) *Biochim. Biophys. Acta* **1359,** 97–109
5. Tilney, L. G., Bonder, E. M., Coluccio, L. M., and Mooseker, M. S. (1983) *J. Cell Biol.* **97,** 112–124
6. Pollard, T. D., and Cooper, J. A. (1984) *Biochemistry* **23,** 6631–6641
7. Pring, M., Weber, A., and Bubb, M. R. (1992) *Biochemistry* **31,** 1827–1836
8. Pantaloni, D., and Carlier, M. F. (1993) *Cell* **75,** 1007–1014
9. Korenbaum, E., Nordberg, P., Björkegren-Sjögren, C., Schutt, C. E., Lindberg, U., and Karlsson, R. (1998) *Biochemistry* **37,** 9274–9283
10. Kang, F., Purich, D. L., and Southwick, F. S. (1999) *J. Biol. Chem.* **274,** 36963–36972
11. Markey, F., Larsson, H., Weber, K., and Lindberg, U. (1982) *Biochim. Biophys. Acta* **704,** 43–51
12. Huxley, H. E. (1963) *J. Mol. Biol.* **7,** 281–308
13. Schutt, C. E., Myslik, J. C., Rozycki, M. D., Goonesekere, N. C., and Lindberg, U. (1993) *Nature* **365,** 810–816
14. Mockrin, S. C., and Korn, E. D. (1980) *Biochemistry* **19,** 5359–5362
15. Goldschmidt-Clermont, P. J., Machesky, L. M., Doberstein, S. K., and Pollard, T. D. (1991) *J. Cell Biol.* **113,** 1081–1089
16. Selden, L. A., Kinosian, H. J., Estes, J. E., and Gershman, L. C. (1999) *Biochemistry* **38,** 2769–2778
17. Hajkova, L., Nyman, T., Lindberg, U., and Karlsson, R. (2000) *Exp. Cell Res.* **256,** 112–121
18. Gutsche-Perelroizen, I., Lepault, J., Ott, A., and Carlier, M. F. (1999) *J. Biol. Chem.* **274,** 6234–6243
19. Lindberg, U., Schutt, C. E., Hellsten, E., Tjader, A. C., and Hult, T. (1988) *Biochim. Biophys. Acta* **967,** 391–400
20. Rozycki, M., Schutt, C. E., and Lindberg, U. (1991) *Methods Enzymol.* **196,** 100–118
21. Grabarek, Z., and Gergely, J. (1990) *Anal. Biochem.* **185,** 131–135
22. Carraway, K. L., and Triplett, R. B. (1970) *Biochim. Biophys. Acta* **200,** 564–566
23. Blikstad, I., Markey, F., Carlsson, L., Persson, T., and Lindberg, U. (1978) *Cell* **15,** 935–943
24. Schüler, H., Korenbaum, E., Schutt, C. E., Lindberg, U., and Karlsson, R. (1999) *Eur. J. Biochem.* **265,** 210–220
25. Kinosian, H. J., Selden, L. A., Estes, J. E., and Gershman, L. C. (1993) *J. Biol. Chem.* **268,** 8683–8691
26. Sugino, Y., and Miyoshi, Y. (1964) *J. Biol. Chem.* **239,** 2360–2364
27. Spudich, J. A. (1974) *J. Biol. Chem.* **249,** 6013–6020
28. Chik, J. K., Lindberg, U., and Schutt, C. E. (1996) *J. Mol. Biol.* **263,** 607–623
29. Otwinowski, Z., and Minor, W. (1997) *Methods Enzymol.* **276,** 307–326
30. Vandekerckhove, J. S., Kaiser, D. A., and Pollard, T. D. (1989) *J. Cell Biol.* **109,** 619–626
31. Larsson, H., and Lindberg, U. (1988) *Biochim. Biophys. Acta* **953,** 95–105
32. Schüler, H., Lindberg, U., Schutt, C. E., and Karlsson, R. (2000) *Eur. J. Biochem.* **267,** 476–486
33. Tanaka, M. a. S., H. (1985) *Eur. J. Biochem.* **151,** 291–297
34. Björkegren, C., Rozycki, M., Schutt, C. E., Lindberg, U., and Karlsson, R. (1993) *FEBS Lett.* **333,** 123–126
35. Mahoney, N. M., Janmey, P. A., and Almo, S. C. (1997) *Nat. Struct. Biol.* **4,** 953–960
36. Perelroizen, I., Carlier, M. F., and Pantaloni, D. (1995) *J. Biol. Chem.* **270,** 1501–1508
37. Tobacman, L. S., and Korn, E. D. (1982) *J. Biol. Chem.* **257,** 4166–4170
38. Valentin-Ranc, C., and Carlier, M. F. (1989) *J. Biol. Chem.* **264,** 20871–20880
39. Kabsch, W., Mannherz, H. G., Suck, D., Pai, E. F., and Holmes, K. C. (1990) *Nature* **347,** 37–44
40. Brenner, S. L., and Korn, E. D. (1980) *J. Biol. Chem.* **255,** 841–844
41. Schüler, H. (2000) *The Molecular Dynamics of Actin*. Ph.D. thesis, Stockholm University, Stockholm
42. Kinosian, H. J., Selden, L. A., Gershman, L. C., and Estes, J. E. (2000) *Biochemistry* **39,** 13176–13188
43. Chen, X., Peng, J., Pedram, M., Swenson, C. A., and Rubenstein, P. A. (1995) *J. Biol. Chem.* **270,** 11415–11423
44. Strzelecka-Golaszewska, H., Moraczewska, J., Khaitlina, S. Y., and Mossakowska, M. (1993) *Eur. J. Biochem.* **211,** 731–742
45. Page, R., Lindberg, U., and Schutt, C. E. (1998) *J. Mol. Biol.* **280,** 463–474
46. West, J. J., Nagy, B., and Gergely, J. (1967) *J. Biol. Chem.* **242,** 1140–1145
47. Kaiser, D. A., Sato, M., Ebert, R. F., and Pollard, T. D. (1986) *J. Cell Biol.* **102,** 221–226
48. Holmes, K. C., Popp, D., Gebhard, W., and Kabsch, W. (1990) *Nature* **347,** 44–49
49. Lorenz, M., Popp, D., and Holmes, K. C. (1993) *J. Mol. Biol.* **234,** 826–836
50. Cedergren-Zeppezauer, E. S., Goonesekere, N. C., Rozycki, M. D., Myslik, J. C., Dauter, Z., Lindberg, U., and Schutt, C. E. (1994) *J. Mol. Biol.* **240,** 459–475
51. Jones, T. A., Zou, J. Y., Cowan, S. W., and Kjeldgaard. (1991) *Acta Crystallogr. A* **47,** 110–119
52. Sayle, R., and Milner-White, E. J. (1995) *Trends Biochem. Sci.* **20,** 374–376